International Journal of Scientific & Engineering Research Volume 8, Issue 10, October-2017

ISSN 2229-5518

Molecular structure, Potentiometric studies of chenodeoxycholic acid and its metal complexes

M.A. Hussien[1], A.A. El-Bindary[2], A.Z. El-Sonbati[2], Y.G. Akawy[1]*

Abstract— Complexes of Mn(II), Co(II), Cu(II) and Zn(II) with 3α,7α-dihydroxy-5β-cholan-24-oic acid have been synthesized. The complexes were characterized. Proton–ligand dissociation constants for ML_1, ML_2 stability constants at room temperature. The selected geometrical structure of the investigated ligand and its metal complexes are calculated by optimizing their bond length and bond angles.

Keywords—Chenodeoxycholic acid; Molecular structure; Potentiometry.

1 Introduction

Chenodeoxycholic acid is a bitter-tasting white powder consisting of crystalline and amorphous particles. It is freely soluble in methanol, acetone and acetic acid and practically insoluble in water [1,2]. It is also known as chenocholic acid, Chenodiol or Chenic Acid. The metal carboxylate have emerged as an important family in the last few years. This family includes not only mono-and dicarboxylates of transition, rare earth, and main-group metals, but also a variety of hybrid structure. Some of the carboxylate possess novel adsorption and magnetic properties. Bile acids (BAs) are a group of water-soluble steroids formed during the catabolism of cholesterol, and synthesised in the hepatocytes of the liver. The products, cholic acid (CA), and chenodeoxycholic acid (CDCA), are called primary bile acids [3].

2. Experimental

2.1. Materials

All the metal salt and solvents used were purchased from Aldrich and Sigma and used as received without further purification, and The ligand used was purchased from International Drug agency for pharmaceutical Industry (IDI).

.

2.2 Preparation of metal complexes

Hot methanolic solution of corresponding metal salts (0.01 mol) was mixed with hot methanolic solution of the ligand (0.02 mol), then adjusted pH of the mixture at 8. The mixture was concentrated by evaporation. The precipitate metal complex were filtered off, washed with acetone and then dried by air

[1]Chemistry Department, Faculty of Science, University of Port Said, Egypt

[2]Chemistry Department, Faculty of Science, University of Damietta, Damietta 34517, Egypt

*Corresponding author: E-mail: yasmeen.gamal40 @yahoo.com (Y.G. Akawy)

2.3 Measurements.

The calculations of geometry optimization were performed using Perkin Elmer ChemBio 3D software by HF method with 3-21G basis set [4]. Geometry optimization option was employed to obtain the most stable structure.

3 Results and Discussion

3.1. Molecular structure of the ligand (HL) and its metal complexes

The selected geometrical structure of the investigated ligand and its metal complexes are calculated by optimizing their bond length and bond angles. The surface of frontier molecular orbital theory (FMOs) is shown in Fig. 1 and 2. The highest occupied molecular orbital (HOMO) and lowest unoccupied molecular orbital (LUMO) energy gaps, ΔE, which is an important stability index, applied to develop theoretical barriers in many molecular systems. The smaller is the value of ΔE, the more is the reactivity of the compound has the calculated quantum chemical parameters are given in (Table 1). Additional parameters such as ΔE, absolute hardness, η, absolute softness, σ, global electrophilicity, ω global softness, S and additional electronic charge, ΔN_{max} have been calculated according to the following Equations (2-8) [5]. The bond length and bond angles of the ligand (HL) and its metal complexes are presented in (Tables 2-6).

$$\Delta E = E_{LUMO} - E_{HOMO} \quad (1)$$

$$\chi = \frac{-(E_{HOMO} + E_{LUMO})}{2} \quad (2)$$

$$\eta = \frac{E_{LUMO} - E_{HOMO}}{2} \quad (3)$$

$$\sigma = 1/\eta \quad (4)$$

$$Pi = -\chi \quad (5)$$

$$S = \frac{1}{2\eta} \quad (6)$$

$$\omega = Pi^2 / 2\eta \quad (7)$$

$$\Delta N_{max} = -Pi/\eta \quad (8)$$

Table 1. The calculated quantum chemical parameters for the ligand and their metal complexes.

Comp.	E_{HOMO} (eV)	E_{LUMO} (eV)	Δ E (eV)	X (eV)	η (eV)	δ(eV)	Pi (eV)	S (eV)	Ω (eV)	ΔN_{max}
HL	-12.45	-0.372	12.075	6.4095	6.0375	0.1656	-6.409	3.018	3.4022	1.061
$[Mn L_2].3H_2O$ (1)	-12.43	-10.87	1.559	11.6505	0.7795	1.2828	-11.65	0.389	5.825	14.94
$[Co L_2].3H_2O$ (2)	-1.091	0.094	1.185	0.4985	0.5925	1.6877	-0.49	0.296	0.249	0.841
[Cu L_2.5H_2O (3)	-7.233	-3.293	3.94	5.263	1.97	0.5076	-5.263	0.98	2. 631	2.6
$[Zn L_2].3H_2O$ (4)	-11.12	-0.541	10.574	5.828	5.287	0. 1891	-5. 828	2.64	2.914	1.10

Table 2. Bond angles of bond length of (HL).

Bond length		Bond angle	
Atoms	Actuel	Atoms	Actual
O(28)-H(68)	0.971	H(68)-O(28)-C(18)	108.250
C(18)-O(28)	1.348	O(28)-C(18)-O(27)	121.692
C(18)-O(27)	1.207	O(28)-C(18)-C(17)	111.566
C(8)-O(9)	1.410	O(27)-C(18)-C(17)	126.740
C(3)-O(4)	1.409	H(44)-O(9)-C(8)	110.282
		H(43)-C(8)-O(9)	105.845
		C(10)-C(8)-O(9)	111.865
		O(9)-C(8)-C(7)	107.025
		H(37)-O(4)-C(3)	109.219
		H(36)-C(3)-O(4)	106.187
		C(5)-C(3)-O(4)	109.716
		O(4)-C(3)-C(2)	109.808

Table 3. Bond length and Bond angels of $[Mn(L)_2].3H_2O$ complex.

Bond length		Bond angels	
Atmos	Actual	Atoms	Actual
Mn(63)-O(65)	1.857	H(141)-O(65)-Mn(63)	99.506
Mn(63)-O(64)	1.856	H(140)-O(65)-Mn(63)	98.978
O(59)-Mn(63)	1.846	H(139)-O(64)-Mn(63)	105.888
O(28)-Mn(63)	1.846	H(138)-O(64)-Mn(63)	100.462
O(27)-Mn(63)	1.813	O(65)-Mn(63)-O(64)	96.934
O(58)-Mn(63)	1.816	O(65)-Mn(63)-O(59)	95.773
		O(64)-Mn(63)-O(59)	136.215
		O(59)-Mn(63)-O(28)	97.553
		O(28)-Mn(63)-O(27)	63.521
		O(28)-Mn(63)-O(58)	130.171
		O(27)-Mn(63)-O(58)	152.905
		Mn(63)-O(58)-C(49)	107.562

Table 4. Bond length and Bond angels of $[Co(L)_2].3H_2O$ complex.

Bond length		Bond angles	
Atoms	Actual	Atoms	Actual
Co(63)-O(65)	1.269	H(141)-O(65)-Co(63)	120.055
Co(63)-O(64)	1.267	H(140)-O(65)-Co(63)	119.483
O(59)-Co(63)	1.241	H(139)-O(64)-Co(63)	116.115
O(28)-Co(63)	1.211	H(138)-O(64)-Co(63)	125.184
O(27)-Co(63)	1.170	O(65)-Co(63)-O(64)	83.618
O(58)-Co(63)	1.163	O(65)-Co(63)-O(59)	88.990
		O(64)-Co(63)-O(59)	171.411
		O(59)-Co(63)-O(28)	91.731
		O(28)-Co(63)-O(27)	84.778
		O(28)-Co(63)-O(58)	174.879
		O(27)-Co(63)-O(58)	99.078
		Co(63)-O(28)-C(18)	93.304
		Co(63)-O(27)-C(18)	108.030

Table 5. Bond length and Bond angels of $[Cu(L)_2].5H_2O$ complex.

Bond length		Bond angels	
Atom	Actual	Atom	Actual
Cu(63)-O(65)	1.850	H(142)-O(65)-Cu(63)	92.491
Cu(63)-O(64)	1.851	H(141)-O(65)-Cu(63)	165.779
O(59)-Cu(63)	1.849	H(140)-O(64)-Cu(63)	165.203
O(28)-Cu(63)	1.848	H(139)-O(64)-Cu(63)	92.065
O(27)-Cu(63)	1.815	O(65)-Cu(63)-O(64)	149.631
O(58)-Cu(63)	1.813	O(65)-Cu(63)-O(59)	89.556
		O(65)-Cu(63)-O(28)	99.587
		O(65)-Cu(63)-O(27)	82.547
		O(65)-Cu(63)-O(58)	105.337
		O(64)-Cu(63)-O(59)	88.213
		O(64)-Cu(63)-O(28)	96.279
		O(64)-Cu(63)-O(27)	81.673
		O(64)-Cu(63)-O(58)	100.657
		O(59)-Cu(63)-O(28)	152.362
		O(59)-Cu(63)-O(27)	144.117
		O(59)-Cu(63)-O(58)	63.418
		O(28)-Cu(63)-O(27)	63.401
		O(28)-Cu(63)-O(58)	88.971
		O(27)-Cu(63)-O(58)	152.306
		Cu(63)-O(59)-C(49)	95.912
		Cu(63)-O(58)-C(49)	107.539
		Cu(63)-O(28)-C(18)	95.974
		Cu(63)-O(27)-C(18)	107.507

Table 6. Bond length and Bond angels of $[Zn(L)_2].3H_2O$ complex .

Bond lengths		Bond angle	
Atoms	Actual	Atoms	Actual
Zn(63)-O(65)	1.890	H(142)-O(65)-Zn(63)	120.000
Zn(63)-O(64)	1.890	H(141)-O(65)-Zn(63)	120.000
O(59)-Zn(63)	1.890	H(140)-O(64)-Zn(63)	120.000
O(28)-Zn(63)	1.890	H(139)-O(64)-Zn(63)	120.000
O(27)-Zn(63)	1.890	O(65)-Zn(63)-O(64)	20.465
O(58)-Zn(63)	1.890	O(65)-Zn(63)-O(59)	54.528
		O(65)-Zn(63)-O(28)	170.523
		O(65)-Zn(63)-O(27)	87.230
		O(65)-Zn(63)-O(58)	69.040
		O(64)-Zn(63)-O(59)	74.632
		O(64)-Zn(63)-O(28)	164.682
		O(64)-Zn(63)-O(27)	77.729
		O(64)-Zn(63)-O(58)	60.861
		O(59)-Zn(63)-O(28)	120.000
		O(59)-Zn(63)-O(27)	120.000
		O(59)-Zn(63)-O(58)	90.000
		O(28)-Zn(63)-O(27)	90.000
		O(28)-Zn(63)-O(58)	120.000
		O(27)-Zn(63)-O(58)	120.000
		Zn(63)-O(59)-C(49)	39.486
		Zn(63)-O(58)-C(49)	90.000
		H(108)-O(35)-C(34)	106.900
		H(107)-C(34)-O(35)	105.429
		Zn(63)-O(28)-C(18)	70.158
		Zn(63)-O(27)-C(18)	90.000

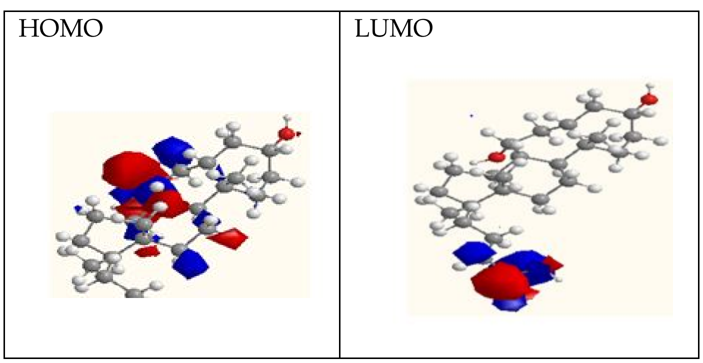

Fig. 1. Molecular structure of the ligand (HL)

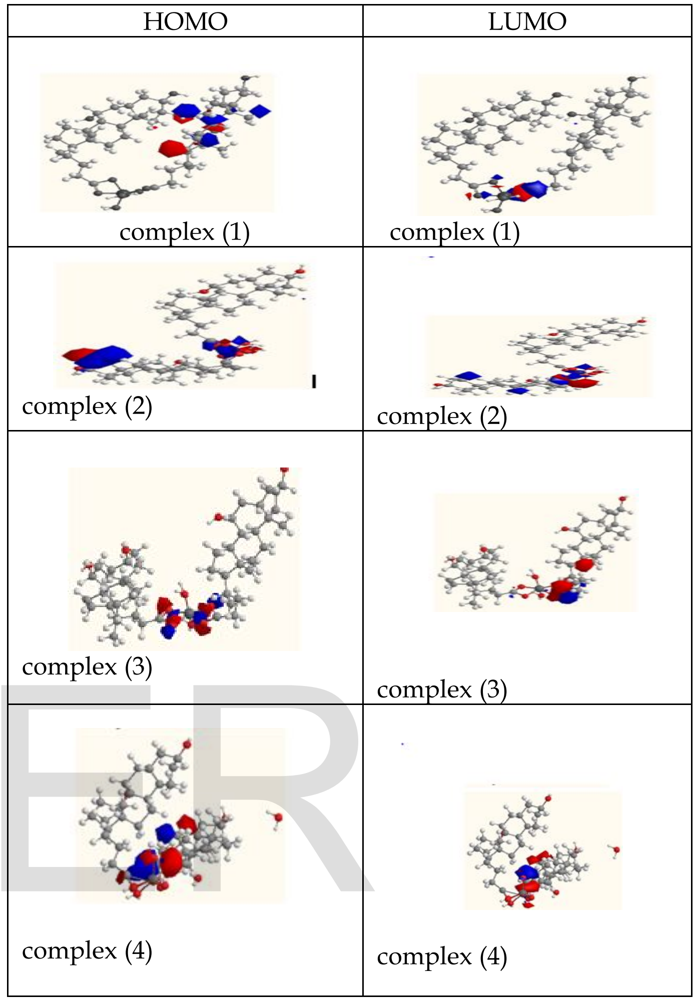

Fig. 2. Molecular structure of the metal complexes

3.2. Potentiometric studies

The interaction of a metal with an electron donor atom of a ligand is usually followed by the release of H^+. Alkaline potentiometric titrations are based on the detection of the protons released upon complexation. The main advantage of this technique, compared to other methods is that from the titration curves it is possible to follow complexation continuously as a function of pH and to detect exactly at which pH complexation takes place. Furthermore, it is possible to calculate the pK_a values, the dissociation constant and the stability constants [6]. The following equilibria were used for the determination of the pK_a values and the stability constants:

$$HL = L^- + H^+$$

$$HL + M^{2+} = ML + H^+$$

$$HL + ML = ML_2^{2-} + H^+$$

HL represents an chenodeoxycholic acid molecule, which bears one dissociable H^+, while M^{2+} are divalent metal ions.

The average number of the protons associated with the reagent molecule, $\bar{n}_A$, was determined at different pH values applying the following Eq. 9:

ISSN 2229-5518

$$\bar{n}_A = Y + \frac{(V_1 - V_2)(N^\circ + E^\circ)}{(V^\circ + V_1)\, TC^\circ_L}$$

where Y is the number of available protons in chenodeoxycholic acid (Y=1) and V_1 and V_2 are the volumes of alkali required to reach the same pH on the titration curve of hydrochloric acid and reagent, respectively, V° is the initial volume (50 cm^3) of the mixture, TC°_L is the total concentration of the reagent, N° is the normality of the sodium hydroxide solution and E° is the initial concentration of the free acid. The titration curves ($\bar{n}_A$ vs. pH) for the proton-ligand systems were constructed and found to extend between 0 and 1 on the $\bar{n}_A$ scale. This means that HL has one dissociable protons (the enolizedhydrogen ionof the carboxylic group, pK_1^H). Different compututional methods [7] were applied to evaluate the dissociation constant. Three replicate titrations were performed; the average value (pKa) obtained are 4.95 at 25 °C.

The formation curves for the metal complexes were obtained by plotting the average number of ligands attached per metal ions ($\bar{n}$) *vs.* the free ligand exponent (pL), according to Irving and Rossotti[8]. The average number of the reagent molecules attached per metal ion, $\bar{n}$, and free ligand exponent, pL, can be calculated using the Eqs. 10 and 11:

$$\bar{n} = \frac{(V_3 - V_2)(N^\circ + E^\circ)}{(V^\circ + V_2)\, \bar{n}_A\, TC^\circ_M}$$

And

$$p = lo_1 \frac{\sum_{n=0}^{n=J} \beta^H_n \left(\frac{1}{[} \right)^n}{T^\circ_L - \bar{n}\; T^\circ_M} \cdot \frac{V^\circ + V_3}{V^\circ}$$

where TC°_M is the total concentration of the metal ion present in the solution, β^H_n is the overall proton-reagent stability constant. V_1, V_2 and V_3 are the volumes of alkali required to reach the same pH on the titration curves of hydrochloric acid, organic ligand and complex, respectively. These curves were analyzed and the successive stability constants were determined using different computational methods [9,10]. The values of the stability constants (log K_1 and log K_2) are given in Tables 10-12. The following general remarks can be made:

i) The maximum value of $\bar{n}$ was ~2 indicating the formation of 1:1 and 1:2 (metal:ligand) complexes only [11].

ii) The metal ion solution used in the present study was very dilute (2 x 10^{-5} M), hence there was no possibility of formation of polynuclear complexes [12, 13].

iii) The metal titration curves were displaced to the right-hand side of the ligand titration curves along the volume axis, indicating proton release upon complex formation of the metal ion with the ligand. The large decrease in pH for the metal titration curves relative to ligand titration curves point to the formation of strong metal complexes [14, 15].

iv) For the same ligand at constant temperature, the stability of the chelates increases in the order Mn^{2+}, Co^{2+}, Ni^{2+} and Cu^{2+} [16-18]. This order largely reflects that the stability of Cu^{2+} complexes are considerably larger as compared to other metals of the 3d series. Under the influence of both the polarizing ability of the metal ion [19] and the ligand field, Cu^{2+} will receive some extra stabilization due to tetragonal distortion of octahedral symmetry in its complexes. The greater stability of Cu^{2+} complexes is produced by the well known *Jahn–Teller* effect [20,21].

Table 7**.** Stepwise stability constants for ML_1 and ML_2 complexes of HL in 40 % (by volume) ethanol-water mixture and 0.1 M KCl at 25 °C.

Comp.	M^{n+}	25 °C	
		log K_1	log K_2
HL	Mn^{2+}	6.50	5.50
	Co^{2+}	6.60	5.60
	Ni^{2+}	6.72	5.70
	Cu^{2+}	6.88	5.95

Referance

[1] C.M. Carey, Editorial, N. Engl. J. Med., 293(24) (1975) 1255.

[2] M . Makishima, A.Y. Okamoto, J.J. Repa, H .Tu, R.M. Learned, A. Luk,

[3] G. Jenkins and L.J. Hardlie., Roy. Soci. Chem., (2008).

[4] V.L. Siji, M.R. SudarsanaKumar, S. Suma and M.R. Prathapachandra-Kurup, Spectrochim. Acta A 76 (2010) 22–28.

[5] A.Z. El-Sonbati, M.A. Diab, A.A. El-Bindary and Sh.M. Morgan, Spectrochim. Acta A 127 (2014) 310-328.

[6] F. Dallavalle, G. Folesani, A. Sabatini, M. Tegoni and A. Vacca, Polyhedron, 20 (2001) 103.

[7] H. Irving and H.S. Rossotti, J. Chem. Soc., (1954) 2904.

[8] H. Irving and H.S. Rossotti, J. Chem. Soc., (1953) 3397.

[9] F.J.C. Rossotti and H.S. Rossotti, Acta Chem. Scand., 9 (1955) 1166.

[10] M.T. Beck and I. Nagybal, Wiley, New York, 1990.

[11] A.A.A. Boraei and N.F.A. Mohamed, J. Chem. Eng. Data, 47 (2002) 987.

[12] P. Sanyal and G.P. Sengupta, Anil. J. Ind. Chem. Soc., 67 (1990) 342.

[13] S. Sridhar, P. Kulanthaipandi, P. Thillai, V. Thanikachalam and G. Manikandan, World J. Chem., 4 (2009) 133.

[14] V.D. Athawale and V. Lele, J. Chem. Eng. Data, 41 (1996) 1015.

[15] V. D. Athawale and S. S. Nerkar, Monatsh. Für Chem., 131 (2000) 267.

[16] F.A.A. Tirkistani and A.A. El-Bindary, Bull. Electrochem., 21 (2005) 265.

[17] G.A. Ibañez and G.M. Escandar, Polyhedron, 17 (1998) 4433.

[18] W.U. Malik, G.D. Tuli and R.D.Madan, 3rd Edition, S. Chand & Company LTD, New Delhi, 1984.

[19] F.R. Harlly, R.M. Burgess and R.M. Alcock, "Solution Equilibria", p. 257, Ellis Harwood, Chichester, 1980.

[20] L.E. Orgel, "An Introduction to Transition Metal Chemistry Ligand Field Theory", p. 55, Methuen, London, 1966.

[21] A. Bebot-Bringaud, C. Dange, N. Fauconnier and C. Gerard, J. Inorg. Biochem., 75 (1999) 71.